Beryllium Dimer: A Bond Based on Non-Dynamical Correlation

ARTICLE *in* THE JOURNAL OF PHYSICAL CHEMISTRY A · MAY 2014

Impact Factor: 2.69 · DOI: 10.1021/jp503145u

THE JOURNAL OF PHYSICAL CHEMISTRY A

Article

pubs.acs.org/JPCA

Beryllium Dimer: A Bond Based on Non-Dynamical Correlation

Muammar El Khatib,[†] Gian Luigi Bendazzoli,*[,‡] Stefano Evangelisti,[†] Wissam Helal,[§] Thierry Leininger,[†] Lorenzo Tenti,[∥] and Celestino Angeli[∥]

[†]Laboratoire de Chimie et Physique Quantiques, Université Paul Sabatier, 118, Route de Narbonne, F-31062 Toulouse Cedex, France

[‡]Dipartimento di Chimica Industriale Toso Montanari, Università degli Studi di Bologna, Viale Risorgimento 4, I-40136 Bologna, Italy

[§]Department of Chemistry, University of Jordan, Amman 11942, Jordan

[∥]Dipartimento di Scienze Chimiche e Farmaceutiche, Università degli Studi di Ferrara, Via Fossato di Mortara 17, I-44121 Ferrara, Italy

S *Supporting Information*

ABSTRACT: The bond nature in beryllium dimer has been theoretically investigated using high-level *ab initio* methods. A series of ANO basis sets of increasing quality, going from sp to spdf ghi contractions, has been employed, combined with HF, CAS-SCF, CISD, and MRCI calculations with several different active spaces. The quality of these calculations has been checked by comparing the results with valence Full-CI calculations, performed with the same basis sets. It is shown that two quasi-degenerated partly occupied orbitals play a crucial role to give a qualitatively correct description of the bond. Their nature is similar to that of the edge orbitals that give rise to the quasi-degenerated singlet−triplet states in longer beryllium chains.[1]

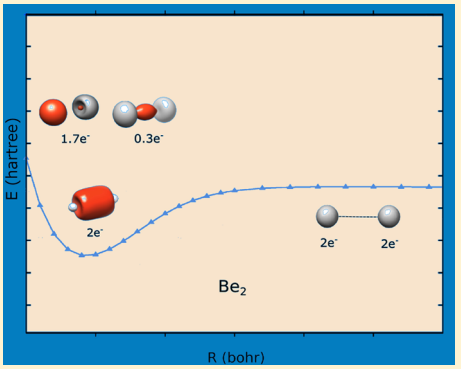

1. INTRODUCTION

Despite a large number of experimental and theoretical investigations on the subject, the bond nature in beryllium dimer is not completely understood. Beryllium, the lightest alkaline-earth-metal element, is a metallic divalent species, whose isolated atom has a closed-shell electronic structure, $1s^2 2s^2$, somehow similar to that of a rare gas. Indeed, beryllium atom has a relatively large ionization potential (899.4 kJ mol^{-1}), and the isolated atom does not support any stable anionic state. However, the empty 2p orbitals are close in energy to the occupied 2s one.[2] For this reason, and because it has two valence electrons, beryllium is able to form two collinear sp-hybridized molecular bonds. This is the case, for instance, of the experimentally well-known linear species BeH_2.

Since 1984, it is known that beryllium is able to form a stable dimer in the gas phase.[3−5] However, the bond in Be_2 is extremely weak, the experimental bond energy being ≈935 cm^{-1} or ≈2.67 kcal/mol, while, at the same time, this species has an unusually long bond length of ≈4.7 bohr.[6,8] In fact, for a long while, the beryllium dimer has been thought as a typical case of "impossible molecule", and it is still presented in this way in some textbooks.

Be_2 has been the subject of a number of high quality experimental and theoretical investigations, but research essentially aimed to study and model its spectroscopical properties (see, e.g., refs 7−10 and references therein). So, despite their success, the intimate nature of the Be−Be bond in this molecule is not yet completely understood, in the sense that a more chemical picture of the bond is desirable. A first step in this direction is the analysis of the Be−Be bond in Be_2 presented by Sheng et al. in ref 11. It is based on a comparison of *ab initio* SCF computations with an sp basis set with the potential curve computed by Patkowski et al.[9] The bond formation is attributed to the s−p hybridization and correlation, but the latter was not analyzed further.

To proceed toward a deeper understanding of the formation of the bond in Be_2, we recall some remarkable features of the Be_2 energy curve to be explained:

1. RHF and associated single-reference methods (CISD, CCSD) are unable to give a correct behavior of the potential-energy surface (PES, actually a curve in our case). This suggests a multireference nature of the bond. In this connection it should be pointed out that to predict the correct shape of the PES, a coupled cluster requires the inclusion of triple excitations as discussed in ref 10.
2. UHF predicts a minimum of the PES, but in the bond region it is heavily spin-contaminated whereas Be_2 is known to be a singlet;

Special Issue: Franco Gianturco Festschrift

Received: April 15, 2014
Revised: May 24, 2014
Published: May 27, 2014

3. As concerns the multireference methods of CAS-SCF(n/m) type, in the following denoted as CAS(n/m) for sake of simplicity, whereas already the small CAS(2/2) PES has the correct shape, rather surprisingly the *full* valence CAS(4/8) PES is clearly *repulsive* in the region of the minimum;
4. The CAS(4/4) PES shows a local minimum, but its energy value is higher than the energy at dissociation;
5. Finally, although the use of the Full-CI approach with large basis sets correctly describes the bond, the FCI energy curve obtained with s and p atomic orbitals only is also repulsive in the region of the minimum.

Because the RHF PES is purely repulsive, it is clear that correlation must play a major role in describing the bond, as already pointed out by Sheng et al.[11] An important point should be kept in mind, in particular when dealing with molecules having very weak bonds: chemistry is a science that deals with energy differences, rather than total energies. This is why, in most cases, the effect of the core electrons can be neglected as a first approximation, although they give by far the largest amount of correlation energy, larger than the correlation due to the valence electrons. Indeed, it is well-known that to achieve full spectroscopical accuracy the effect of core electrons has to be taken into account as we already observed in a previous study of Be_2.[12] However, the present work is not intended to predict accurate values of spectroscopical quantities, but rather to develop a "chemical" picture of the Be−Be bond. For this reason we consider adequate for our purpose to keep the 1s orbitals frozen at the SCF level; this point is further discussed in section 2. More important, when the wave function of the system changes its nature under variation of the parameters governing the system, like the molecular geometry, it is essential to ensure a well balanced accuracy as a function of the parameters. The case of beryllium dimer falls precisely in this category and the energies involved are small on a chemical scale. It turns out that, as it will be discussed in detail later, the nature of Be_2 wave function is very different at the equilibrium distance (R close to 4.6 bohr) and in the large R region ($R \gtrsim 8$ bohr). In particular, it will be shown that the wave function can be expressed essentially as a combination of *two* Slater determinants in the region of the bond, whereas only a *single* determinant is required at dissociation.

Traditionally, the correlation effects are classified into two types, although not clearly distinct, dynamical and non-dynamical correlation, that require different approaches to be treated. In this article, following a largely diffuse classification, we associate the nondynamical correlation to the effect of a quasi-degeneracy, usually restricted to a small number of Slater determinants in the CAS-SCF reference wave function. Dynamical correlation, on the other hand, is related to the *Coulomb Hole* surrounding each electron. Once a suitable reference wave function has been computed, the dynamical correlation is added by considering a very large number of excitations on top of the reference, usually singly and doubly excited determinants in truncated CI, and up to all determinants in the case of FCI. Because this type of energy correlation is the result of a huge amount of extremely small contributions, it converges to the exact limit in a way smoothly dependent upon the molecular geometry. A well balanced treatment of non dynamical correlation, on the other hand, is a more problematic task. Consider, for example, the case when the wave function changes from single to multireference at some geometry: the energy can show a sudden jump. Moreover, it should be stressed that, even if we limit our discussion to variationally bounded methods, the philosophy "the lowest the better" is not necessarily correct. Indeed, one can have a wave function whose Non Parallelism Error (NPE) with respect to the exact limit is much smaller than that of a wave function whose total energy is lower.

Coming back to the Be_2 case, the fact that a wave function does not show an energy well at the right distance can be due to the reference wave function not containing the crucial determinants needed to describe the bond. Furthermore, it is also possible that, at the considered level of theory, the amount of correlation energy added at dissociation is larger than that added at the equilibrium. Because of the flatness of the minimum, even a tiny difference is sufficient to hide the well. In this article, we will present results on the Be_2 potential energy curves computed at different *ab initio* levels of theory, as well as basis-set and active-space effects to better understand the electronic structure of this molecule. Once we have explained the formation of the minimum in the PES, further insight about the nature of the Be−Be bond is provided by the total position spread (TPS).[13−20] This quantity has been shown to be very useful as an indicator of the nature of the wave function and bond formation as shown for diatomics.[17,18] At the same time, it is a powerful tool to monitor the behavior of the electrons in a molecular system.[19,20]

This work is organized as follows: in section 2 the details about the different calculations are presented; Section 3 discusses the UHF PES of Be_2; in section 4 our picture of the Be−Be bond is presented. Basis-set effects, molecular orbitals and active-space effects are presented in sections 4.1, 4.2, and, 4.3 respectively. The TPS is considered in section 4.4, and the last part is devoted to the conclusions.

2. COMPUTATIONAL DETAILS

We employed the high quality correlation-consistent v6zp basis set optimized by Kirk Peterson.[21] It consists of a set of (16s9p5d4f3g2h1i) primitive Gaussian orbitals, contracted to (7s6p5d4f3g2h1i). Different truncations were obtained by discarding the higher angular moment functions of the complete contracted basis set. Thus, the following contractions and notations were used along this investigation: sp (7s6p), spd (7s6p5d), spdf (7s6p5d4f), spdfg (7s6p5d4f3g), spdfgh (7s6p5d4f3g2h), and finally spdfghi (7s6p5d4f3g2h1i). These bases are the same as those used in a previous study of Be_2.[12]

The *ab initio* methods range from HF-SCF, CAS, CISD, MRCI, and FCI. We adopt the notation MRCI(n,m) to indicate a single−double CI performed on the CAS(n/m) wave function. Accordingly, MRCI(0,0) is a synonimous of CISD, but in this case we prefer the latter and use MRCI for the multireference case. The HF-SCF, CAS,[22−24] CISD, and MRCI[25,26] calculations were performed by using the MOLPRO *ab initio* package.[27] FCI calculations, on the other hand, were performed by using the NEPTUNUS FCI code.[28−30] NEPTUNUS is interfaced to the MOLCAS[31] and also to the DALTON[32] packages via the Q5Cost protocol.[33−36] The FCI calculations are actually frozen-core full configuration interaction; the $1\sigma_g$, $1\sigma_u$ core orbitals are kept doubly occupied and frozen at the SCF level. These FCI calculations are actually the same reported in ref 12. The initial Hartree−Fock computations were performed using MOLCAS and DALTON quantum chemistry programs. The obtained one- and two-electron

dx.doi.org/10.1021/jp503145u | J. Phys. Chem. A 2014, 118, 6664−6673

atomic integrals were transformed to the molecular basis set and the NEPTUNUS code[28] was used to compute the FCI wave functions and the total position spread tensor. We recall that all electron FCI computations are feasible only for our very poor bases: the number of symmetry adapted determinants involved by the CI vector is already $\approx 2 \times 10^{12}$ for spd and $\approx 2 \times 10^{14}$ for spdfghi AO basis.

As already pointed out in the Introduction, we do not require full spectroscopical accuracy to our best potential curves that we consider to correctly describe the Be−Be bond. One may wonder how important is the difference with respect to the best ones available in the literature.[7−10] As concerns the values of spectroscopical quantities computed at FCI level with our basis sets, we refer to the discussion in ref 12. As an example we now consider in some detail the FCI curve computed with the spdfg basis which is not our best, but the largest one for which we have a complete set of data. The main deficiency of the PES is a small depth of the potential well: our computed values of D_e with the spdfg and higher bases are about 12% smaller than the best published values by Koput et al.[10] and Meshkov et al.[8] Other spectroscopic quantities (r_e, ω_e, $\omega_e x_e$) show much better agreement with experiment.[12] The quality of the computed PES was also tested by computing the vibrational levels by using Le Roy's program LEVEL.[37] It turns out that this curve supports 12 vibrational levels, although the highest one $v = 11$ is extremely close to the dissociation limit, as can be seen from the Supporting Information. Therefore, we conclude that our best FCI potentials are not as good as the best published, but adequate for our purpose.

3. THE UHF WAVE FUNCTION

Additional evidence in favor of the multireference nature of the Be_2 wave function at equilibrium are provided by UHF calculations. First, it is a remarkable fact that, whereas the singlet RHF curve is completely repulsive, the ROHF triplet has a minimum near $R = 4$ bohr.[12] An accurate theoretical value for the triplet equilibrium distance can be obtained at FCI level, and with the spdfghi basis set, it is 4.6676 bohr.[12] However, these ROHF results show a triplet lying *below* the RHF singlet, contrary to experiment, from which it is known that the singlet is the ground state.

This fact immediately suggests that something is *qualitatively* wrong with the single-determinant RHF description. This is confirmed by the presence, at UHF level, of broken-symmetry ground-state minimum with spin-projection $S_z = 0$, a fact already pointed out by Lepetit and Malrieu a long time ago.[38] We consider here the results obtained with the spdfg basis set. Because of the spin-contamination phenomenon, the UHF wave function is neither a singlet nor a triplet. For instance, at $R = 4.0$ bohr the expectation value of $\hat{S}^2$ is 0.9089 (in au), indicating a UHF wave function composition roughly equal between singlet and triplet at this distance.

The value of the spin contamination of the UHF solution, defined as $\langle \hat{S}^2 \rangle$, is shown in Figure 1. It is close to 1 in the region of the bond and goes down at large distances. Notice, however, that it never goes to zero, indicating an instability of the RHF solution at any distance. This instability, is due, in our opinion, to the low-lying 2p orbitals of the atoms that are close in energy to the 2s orbital. The curve in Figure 1 has a reversed sigmoidal shape, and its center $R \approx 6$ bohr might be considered as marking a nonsharp transition from many to single reference wave function. It roughly coincides with the "anomalous" change of slope of the potential curve of Be_2 pointed out by Li et al.[39] and interpreted by Sheng et al.[11] as the intersection beteween correlation and s−p hybridization energy.

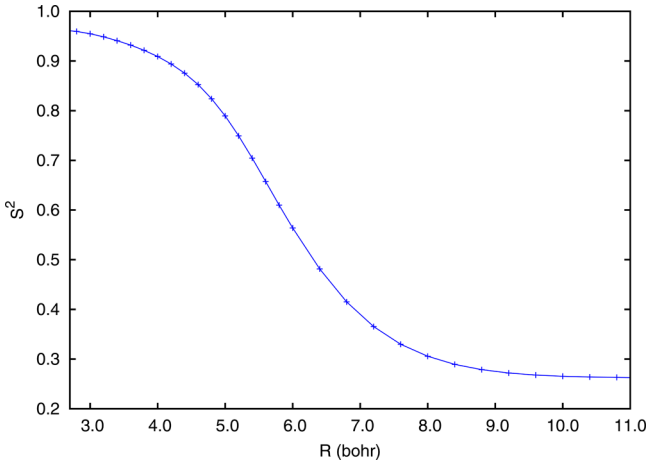

Figure 1. Expectation value of the spin contamination, $\langle \hat{S}^2 \rangle$ (au) as a function of the internuclear distance, R (bohr).

In a schematic description, the UHF solution can be assumed to be a mixture of a singlet $|\Psi_S\rangle$ with a triplet contaminant $|\Psi_T\rangle$, and the singlet is expected to describe the Be_2 ground state. In principle, none of these states can be described by a single-determinant picture. A crude estimate of the energy of the singlet component of the UHF wave function can be obtained as follows. By adopting an argument similar to the one used in density functional theory for the treatment of magnetic systems, one can write

$$|\Psi_{UHF}\rangle = \cos(\theta)\langle\Psi_S| + \sin(\theta)\langle\Psi_T| \quad (1)$$

The mean value of the $\hat{S}^2$ operator in the UHF wave function is given by

$$\langle \hat{S}^2 \rangle = \langle \Psi_{UHF}|\hat{S}^2|\Psi_{UHF}\rangle = 2\sin^2(\theta) \quad (2)$$

and then $\sin^2(\theta) = (1/2)\langle \hat{S}^2 \rangle$. In a similar way, the UHF energy in this scheme is given by

$$E_{UHF} = \cos^2(\theta)E_S + \sin^2(\theta)E_T \quad (3)$$

so that finally one can define the energy of a "reconstructed singlet" as

$$E_S = \left(E_{UHF} - \frac{1}{2}\langle \hat{S}^2 \rangle E_T\right) \Big/ \left(1 - \frac{1}{2}\langle \hat{S}^2 \rangle\right) \quad (4)$$

The triplet energy needed by eq 4 is obtained from a ROHF computation with $S_z = \pm 1$. In Figure 2, the curves of the Closed-Shell RHF for the singlet, the ROHF for the triplet, and the spin-contaminated broken-symmetry UHF (with $S_z = 0$) are reported (spdfg basis set). The energy of the reconstructed singlet, shown in eq 4, is also reported. In the figure. It shows the presence of a many-determinant OS singlet, having an equilibrium distance of about 3.8756 bohr, and a dissociation energy of about 112.572 kJ/mol. These results are clearly not quantitatively satisfactory, but they confirm the multireference nature of the bond in Be_2.

4. THE MULTIREFERENCE PICTURE

For the reasons above it was so far impossible to provide a simple, yet satisfactory picture of the bond formation in Be_2. However, some hint in this direction came to us from recently performed *ab initio* configuration interaction (CI) studies on

dx.doi.org/10.1021/jp503145u | J. Phys. Chem. A 2014, 118, 6664−6673

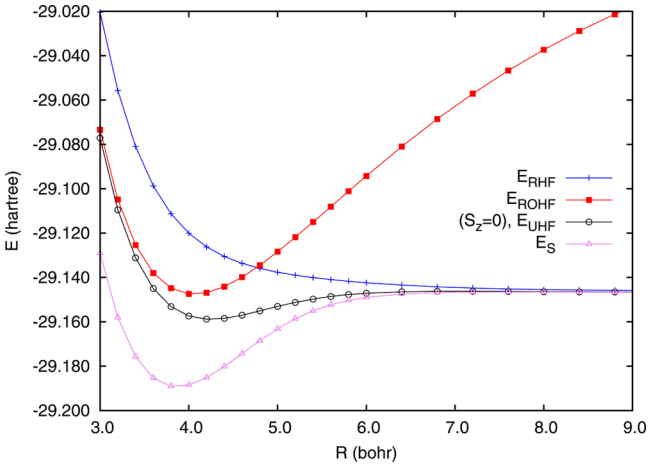

Figure 2. Total energies of Be_2 for the singlet closed-shell at RHF level, the triplet state computed at ROHF level and spin-contaminated broken-symmetry UHF (with $S_z = 0$). The E_s potential energy curve corresponds to the reconstructed singlet as shown in eq 4 in Section 3

linear, equally spaced Be_n structures.[40] In these calculations, aimed to investigate the metal−insulator transition as a function of the internuclear separation R, we evidenced the formation, close to the equilibrium geometries, of two partially occupied edge orbitals. Consequently we found the presence of two quasi-degenerated low-lying states, a singlet and a triplet.[1] In particular, it is remarkable that the singlet−triplet energy splitting in Be_n follows an almost perfect exponential decay as a function of n, *including the case of the dimer*. This suggests the possibility that the structural form of linear Be_n is already present in Be_2 and therefore that the edge orbitals should be taken into account for the description of the electronic structure of this molecule.

For this reason, we performed several types of calculation, in particular in the region of the bond. For convenience, the latter is identified by values of the internuclear distance $R \lesssim 6$ bohr in agreement with the observation in section 3 and will be denoted by BR, whereas AR will denote the asymptotic or dissociation region $R \gtrsim 6$ bohr. Obviously, and as previously pointed out, the transition between the two regions is rather smooth. The results of these calculations in the BR could be rationalized on the basis of a simple MO picture involving the edge orbitals, as described in the following.

Let us consider the beryllium dimer close to its equilibrium distance. The $1\sigma_g$ and $1\sigma_u$ orbitals, coming from the even and odd combination of the 1s core orbitals, respectively, do not participate in a significant way to the bonding mechanism. On the other hand, four valence atomic orbitals play a crucial role to explain the bond. They are, for each atom, the 2s and $2p_z$ orbitals, z being the intermolecular axis. By combining these orbitals, it is possible to build, on each Be atom, two sp hybrid orbitals: one, ρ, pointing toward the other atom, and a second one, τ, pointing in the opposite direction, outside the internuclear region. The even/odd combinations of ρ_A and ρ_B have a clear bonding/antibonding character, respectively, because the two orbitals occupy essentially the same central region of the molecule. The corresponding combinations of τ_A and τ_B, on the other hand, have a much weaker character and give rise to the edge orbitals, quasi-degenerated in longer chains.[1] The sequence (from the lower in energy to the higher) of the six MO's, as discussed later, is the following one:

$$1\sigma_g = 1s_A + 1s_B \quad \text{(core)}$$

$$1\sigma_u = 1s_A - 1s_B \quad \text{(core)}$$

$$2\sigma_g = \rho_A + \rho_B \quad \text{(bonding)}$$

$$2\sigma_u = \tau_A - \tau_B \quad \text{(edge)}$$

$$3\sigma_g = \tau_A + \tau_B \quad \text{(edge)}$$

$$3\sigma_u = \rho_A - \rho_B \quad \text{(antibonding)}$$

Among the valence orbitals, the bonding $2\sigma_g$ orbital is doubly occupied, whereas the antibonding $3\sigma_u$ orbital is empty. Therefore, at a first approximation, the latter orbitals are not expected to be important in the active space of a CAS-SCF calculation. Things are completely different for the "edge orbitals" $2\sigma_u$ and $3\sigma_g$. This is confirmed by their occupation numbers (Table 1). A further confirmation is the fact that, at

Table 1. Orbital Occupation Numbers at R = 4.6 bohr, spdfg Basis Set

orbital	CAS(2/2)	CAS(4/4)	CAS(4/8)
$2\sigma_g$		1.969 91	1.867 88
$2\sigma_u$	1.695 23	1.681 42	1.705 57
$3\sigma_g$	0.304 77	0.320 27	0.171 62
$3\sigma_u$		0.028 40	0.021 29
$1\pi_g$			0.071 20
$1\pi_u$			0.045 62

RHF level, the energy curve of the singlet is purely repulsive. This remains true also when the dynamic correlation is added, at CISD or CC level. (See Figure 3 where, for the sake of comparison with FCI calculations, the CISD energy curve of the singlet is reported).

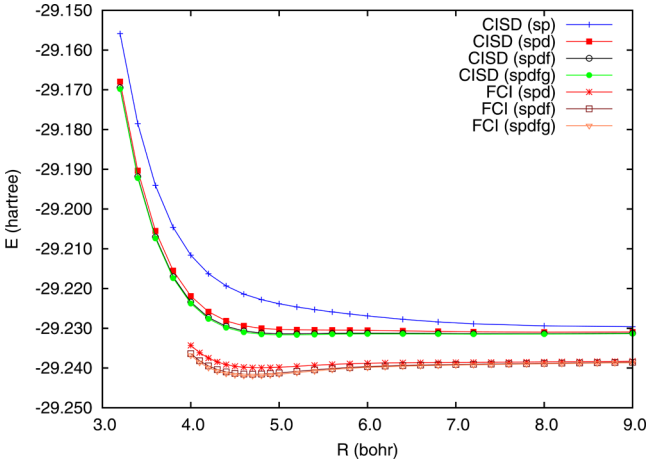

Figure 3. CISD and FCI potential energy surfaces computed with four different basis sets sp, spd, spdf, and spdf g.

It is a remarkable fact that the form of these four orbitals does not depend in a strong way on the spin symmetry of the wave function. Moreover, if the CAS(2/2) singlet−triplet averaged orbitals, or even triplet orbitals, are used to compute the singlet energy curve, a minimum in the region of 4.6 bohr is clearly present. Once the dynamical correlation is added, at CISD level, the singlet curves obtained with different sets of

dx.doi.org/10.1021/jp503145u | J. Phys. Chem. A 2014, 118, 6664−6673

orbitals are almost indistinguishable (see figures in Supporting Information).

In the following subsections, the effect on the PES form of both the basis-set quality and the level of correlation are investigated.

4.1. Basis-Set Effects. The effect of the basis-set quality on the results is first considered. Only energy curves obtained with the four basis sets sp, spd, spdf, and spdfg, which are the only ones for which a complete FCI curve is available, will be displayed in the figures. On the other hand, in the tables we will report also values obtained with the larger spdf gh and spdf ghi basis sets. In particular, these last values (estimated to be a fraction of a kJ/mol off the infinite basis-set limit) will be taken as "reference". From Table 2 and Figure 3 it is seen that the convergence of the FCI values as a function of the basis-set size is much slower at equilibrium than at dissociation, and this effect is particularly pronounced for the small basis sets. In particular, the sp result is about 30 kJ/mol higher than the reference at equilibrium, but only about one-tenth of this value at dissociation. The same thing, although less pronounced, happens with the spd basis set, whereas for larger basis sets the error becomes less than one kJ/mol. This behavior explains the fact that the sp basis set gives a repulsive curve, apart from a very shallow van der Waals minimum at large distance, whereas the well depth for the spd basis set is about only one-half of the reference value.

Table 2. Total Energies ($E(R)$, hartree), Energy Differences ($\Delta_{REF}(R)$, kJ/mol), and Fixed-Distance Dissociation Energies ($D = E(\infty) - E(4.60)$, kJ/mol) of the FCI Wavefunctions, Obtained with the Different Basis Sets[a]

basis set	$E(R)$, $\Delta(R)$	R = 4.60 bohr	$R = \infty$	D
s	$E(R)$	−29.11 494 987	−29.15 317 977	−100.373
	$\Delta_{REF}(R)$	333.733	223.336	
sp	$E(R)$	−29.22 971 567	−29.23 694 647	−18.982
	$\Delta_{REF}(R)$	32.414	3.408	
spd	$E(R)$	−29.23 981 535	−29.23 786 573	5.119
	$\Delta_{REF}(R)$	5.898	0.993	
spdf	$E(R)$	−29.24 153 059	−29.23 810 902	8.983
	$\Delta_{REF}(R)$	1.395	0.354	
spdf g	$E(R)$	−29.24 190 685	−29.23 819 529	9.745
	$\Delta_{REF}(R)$	0.407	0.129	
spdf gh	$E(R)$	−29.24 202 036	−29.23 823 061	9.950
	$\Delta_{REF}(R)$	0.110	0.034	
spdf ghi	$E(R) \equiv E_{REF}(R)$	−29.24 206 189	−29.23 824 376	10.025

[a] $E_{REF}(R)$ is the value of the FCI energy computed with the largest basis set (spdf ghi).

In Table 3, the HF, CISD, and FCI results are shown for the different basis sets. The HF results are virtually converged already with the sp basis set. The correlation energy is much larger than the depth of the energy well. For the beryllium atom (i.e., close to dissociation), the CISD and FCI energies do not depend on the basis set in a strong way, with the partial exception of the sp basis set. The opposite is true close to the equilibrium distance. We report in Table 2 the total energies for a distance of 4.6 bohr and at dissociation. From Figure 3, it is seen that the CISD approach is unable to describe, even in a qualitative way, the equilibrium well of the molecule: at most, in the cases of the spdf and spdf g basis sets, the curve presents a double minimum, the equilibrium well occurring at a slightly larger interatomic distance (∼5.10 bohr).

Table 3. Total Energies ($E(R)$, hartree) and Fixed-Distance Dissociation Energies ($D = E(\infty) - E(4.60)$, kJ/mol) of the HF and CISD Wavefunctions, Respectively, with the Different Basis Sets[a]

basis set	$E(R)$, $\Delta(R)$	R = 4.60 bohr	$R = \infty$	D
sp	$E_{HF}(R)$	−29.13 240 550	−29.14 604 150	−35.801
	$E_{CISD}(R)$	−29.22 140 351	−29.22 951 615	−21.300
	$\Delta_{HF}(R)$	255.488	238.671	
	$\Delta_{CISD}(R)$	21.824	19.510	
spd	$E_{HF}(R)$	−29.13 364 615	−29.14 604 150	−32.544
	$E_{CISD}(R)$	−29.22 939 739	−29.23 067 365	−3.351
	$\Delta_{HF}(R)$	278.747	241.085	
	$\Delta_{CISD}(R)$	27.352	18.883	
spdf	$E_{HF}(R)$	−29.13 369 735	−29.14 604 150	−32.410
	$E_{CISD}(R)$	−29.23 068 539	−29.23 096 317	−0.729
	$\Delta_{HF}(R)$	283.116	241.723	
	$\Delta_{CISD}(R)$	28.474	18.761	
spdf g	$E_{HF}(R)$	−29.13 369 978	−29.14 604 150	−32.403
	$E_{CISD}(R)$	−29.23 099 527	−29.23 106 417	−0.181
	$\Delta_{HF}(R)$	284.098	241.950	
	$\Delta_{CISD}(R)$	28.648	18.723	
spdf gh	$E_{HF}(R)$	−29.13 369 990	−29.14 604 150	−32.401
	$E_{CISD}(R)$	−29.23 109 595	−29.23 110 506	−0.024
	$\Delta_{HF}(R)$	284.395	242.043	
	$\Delta_{CISD}(R)$	28.682	18.708	
spdf ghi	$E_{HF}(R)$	−29.13 369 991	−29.14 604 150	−32.401
	$E_{CISD}(R)$	−29.23 113 340	−29.23 112 005	0.035
	$\Delta_{HF}(R)$	284.504	242.077	
	$\Delta_{CISD}(R)$	28.693	18.703	

[a] $\Delta_{HF}(R)$ and $\Delta_{CISD}(R)$ are the corresponding relative energies with respect to the FCI energy (kJ/mol).

4.2. Molecular Orbitals. In Figure 4, we report the four valence orbitals $2\sigma_g$, $3\sigma_g$, $2\sigma_u$, and $3\sigma_u$, obtained with the spdf g basis set and a CAS(4/4) active space. The $2\sigma_u$ and $3\sigma_g$ orbitals are hardly distinguishable from their CAS(2/2) homologues: for this reason, only the CAS(4/4) valence orbitals are reported in the figure. In Table 1 we report, for the same atomic basis set, the occupation numbers n_{occ} of the natural orbitals of different wave functions and active spaces. Because the orbital

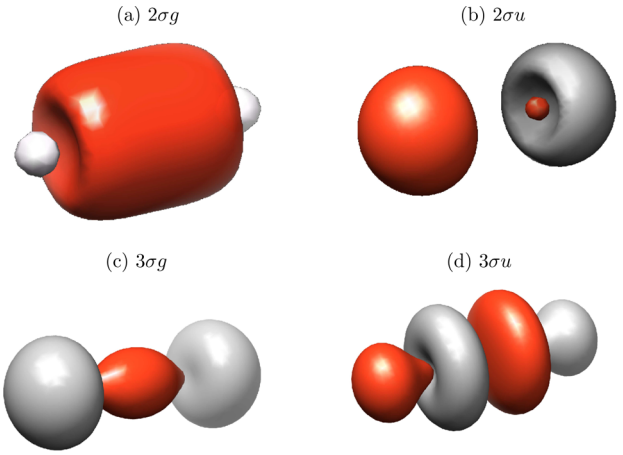

Figure 4. Four valence orbitals $2\sigma_g$, $3\sigma_g$, $2\sigma_u$, and $3\sigma_u$, computed with an active space CAS(4/4) employing the spdf g basis set.

dx.doi.org/10.1021/jp503145u | J. Phys. Chem. A 2014, 118, 6664−6673

energies are not well-defined for CAS wave functions, we will use the acronym HOMO to denote orbitals with high n_{occ}(>1.4) ordered in descending occupation number. Similarly, the acronym LUMO denotes orbitals with low n_{occ}(<1) ordered in ascending occupation. The values in the table clearly show that the HOMO $2\sigma_u$ and LUMO $3\sigma_g$ are the crucial orbitals that must be included in the active space. The HOMO−1 ($2\sigma_g$)/LUMO+1 ($3\sigma_u$) orbitals have a classical bonding/antibonding shape, respectively, showing a maximum/minimum of the orbital density in the region between the two nuclei. On the other hand, the HOMO and LUMO edge orbitals have their largest values in the region external to the molecular bond. To investigate the structure of these orbitals, a localized picture is more appropriate. In Figure 5, the

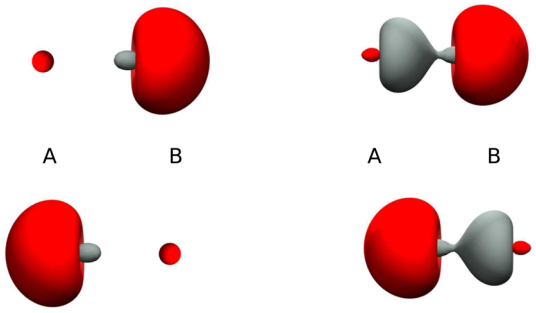

Figure 5. Left: Two pure sp_z hybrid orbitals, pointing outward with respect to the bond: $(2s - 2p_z)/\sqrt{2}$ on atom A and $(2s + 2p_z)/\sqrt{2}$ on atom B. Right: Corresponding CAS(2/2) localized orbitals, given by the linear combinations $(3\sigma \pm 2\sigma_u)/\sqrt{2}$.

combinations $3\sigma_g + 2\sigma_u$ and $3\sigma_g - 2\sigma_u$ are compared with the nonorthogonal pure hybrids τ_A and τ_B. The $3\sigma_g + 2\sigma_u$ and $3\sigma_g - 2\sigma_u$ combinations give two orbitals localized on each atom showing a strong similarity with the hybrids τ_A and τ_B that point outward with respect to the molecular bond.

4.3. Active-Space Effects. The effects of the different levels of correlation contributions will be now considered in detail. For the sake of compactness, only the spdf g basis set will be considered, because this is the largest one for which the results are available at a large number of points. Moreover, the effect of the h and i orbitals accounts for just a few percent of the energy-well depth. For this reason, although these orbitals are certainly important for a quantitative detailed description of the bond, their presence does not change the global picture in a significant manner.

In Table 4 the total energies for a distance of 4.6 bohr and at dissociation, calculated with a CAS(2/2), MRCI(2/2), and at FCI level are reported. In Figure 6, several CAS curves and the corresponding CISD results are shown, obtained using different CAS spaces. In particular, the CAS(0/0), CAS(2/2), CAS(4/4), and CAS(4/8) have been considered: CAS(0/0) is nothing but RHF; CAS(2/2) is obtained by distributing two electrons in the (formally) occupied orbital $2\sigma_u$ and empty orbital $3\sigma_g$; CAS(4/4) is the full valence σ CAS, containing the $2\sigma_g$, $2\sigma_u$, $3\sigma_g$, and $3\sigma_u$ orbitals. Finally, the CAS(4/8) is the full valence CAS, where the empty orbitals $1\pi_g$ and $1\pi_u$ are added to the active space. The different behaviors are better seen in Figures 7 and 8, where the CAS and MRCI results, respectively, are reported, and where the FCI result with the same basis set is also added for comparison.

From Figure 7, it appears how the different contributions to the correlation energy are introduced by the different CAS

Table 4. Total Energies ($E(R)$, in hartree) and Fixed-Distance Dissociation Energies ($D = E(\infty) - E(4.60)$, kJ/mol) of the CAS and MRCI Wavefunctions with the Different Basis Sets[a]

basis set	$E(R)$, $\Delta(R)$	R = 4.60 bohr	$R = \infty$	D
sp	$E_{CAS(2/2)}(R)$	−29.16 300 920	−29.14 859 819	37.836
	$E_{MRCI(2/2)}(R)$	−29.22 482 311	−29.23 015 734	−14.005
	$\Delta_{CAS}(R)$	175.138	231.958	
	$\Delta_{MRCI}(R)$	12.845	17.825	
spd	$E_{CAS(2/2)}(R)$	−29.16 477 689	−29.14 861 221	42.440
	$E_{MRCI(2/2)}(R)$	−29.23 420 378	−29.23 129 937	7.626
	$\Delta_{CAS}(R)$	197.013	234.335	
	$\Delta_{MRCI}(R)$	14.733	17.240	
spdf	$E_{CAS(2/2)}(R)$	−29.16 481 779	−29.14 861 305	42.546
	$E_{MRCI(2/2)}(R)$	−29.23 576 828	−29.23 158 550	10.982
	$\Delta_{CAS}(R)$	201.409	234.972	
	$\Delta_{MRCI}(R)$	15.129	17.128	
spdf g	$E_{CAS(2/2)}(R)$	−29.16 481 980	−29.14 861 305	42.551
	$E_{MRCI(2/2)}(R)$	−29.23 612 482	−29.23 168 538	11.656
	$\Delta_{CAS}(R)$	202.392	235.198	
	$\Delta_{MRCI}(R)$	15.181	17.092	

[a]All values are obtained from a CAS(2/2) active space. $\Delta_{CAS}(R)$ and $\Delta_{MRCI}(R)$ indicate the corresponding energy differences (kJ/mol) with respect to the FCI energy.

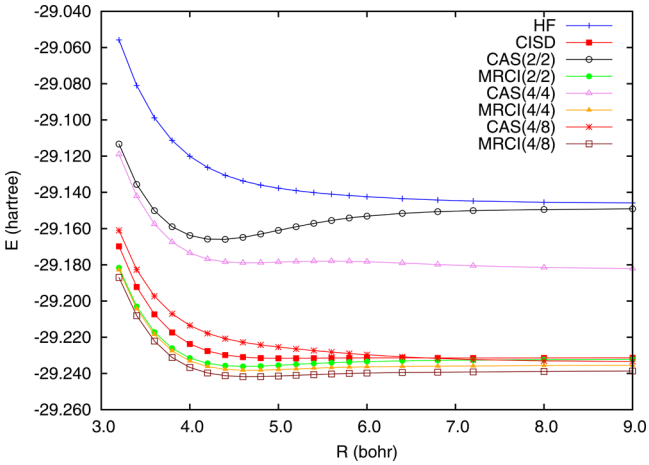

Figure 6. Total energies with different CAS spaces (CAS(0/0)=HF, CAS(2/2), CAS(4/4), and the full valence CAS, CAS(4/8)), spdf g basis sets, together with the corresponding CISD and MRCI results.

spaces in the bond (BR) and dissociation or asymptotic (AR) regions:

1. CAS(0/0)=RHF: The correlation energy is larger in BR than in AR; the curve is repulsive.
2. CAS(2/2): BR starts to be correctly described at reference level; almost no correlation is recovered in AR. The curve has a minimum, but too deep.
3. CAS(4/4): A large fraction of correlation energy is recovered in AR, much less in BR, and the curve becomes repulsive again.
4. CAS(4/8): Essentially the same behavior occurs as in the previous case. The curve is essentially parallel to RHF.

Figure 8 shows the effect of the dynamical correlation introduced by MRCI.

dx.doi.org/10.1021/jp503145u | J. Phys. Chem. A 2014, 118, 6664−6673

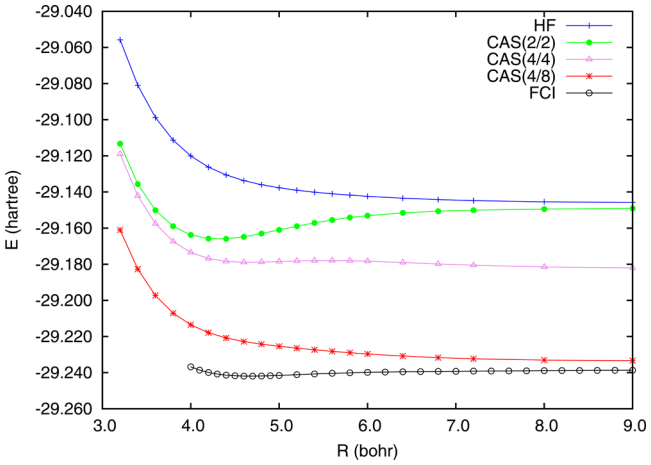

Figure 7. Total energies with different CAS spaces (CAS(0/0)=HF, CAS(2/2), CAS(4/4), and the full valence CAS, CAS(4/8)), spdf g basis sets. The FCI curve obtained with the same basis set is also shown.

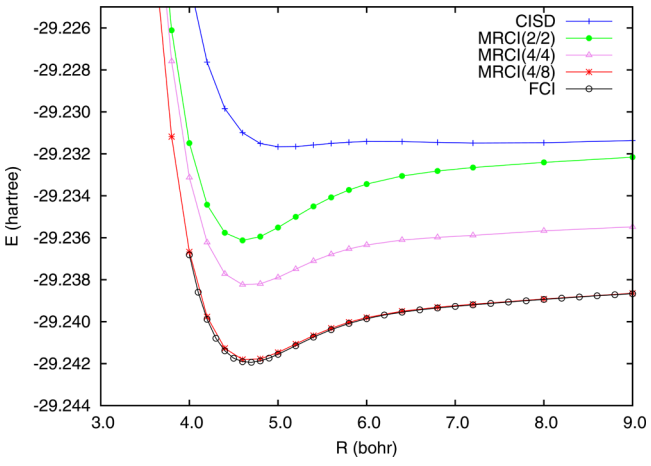

Figure 8. Total CISD energies obtained with different CAS spaces (CAS(0/0)=HF, CAS(2/2), CAS(4/4), and the full valence CAS, CAS(4/8)), spdf g basis sets. The corresponding FCI curve is also shown.

1. The CISD curve is still essentially repulsive, with a spurious maximum in the region 6−6.5 bohr, at the border BR-AR.
2. The MRCI(2,2) does not dissociate correctly, its correlation energy is too small in the AR. As a consequence, the potential well is too deep.
3. The MRCI(4,4) curve is parallel to FCI, implying a well balanced treatment of correlation in BR and AR and a good value of the potential depth.
4. MRCI(4,8) practically coincides with FCI. The difference MRCI(4,4) − MRCI(4,8) is essentially constant in both BR and AR because it is due to the correlation of the π orbitals not partecipating to the bond.

The effect of the AO basis set is illustrated in Figure 9. The main observation is that the dynamical correlation introduced by MRCI shifts down the CAS(2/2) curves, with the exception of the sp basis: the lack of d-orbitals prevents a reasonable evaluation of the dynamical correlation, particularly in the BR.

Finally, in Figure 10, we report the occupation numbers of the HOMO−LUMO edge pair, $2\sigma_u$ and $3\sigma_g$, obtained with the three different active spaces. Their behavior as a function of the

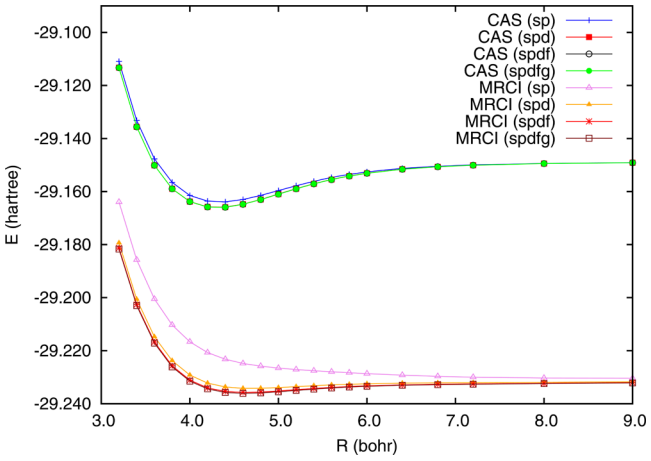

Figure 9. CAS(2/2) total energies and the corresponding MRCI(2/2) results with the different basis sets, sp, spd, spdf, and spdf g.

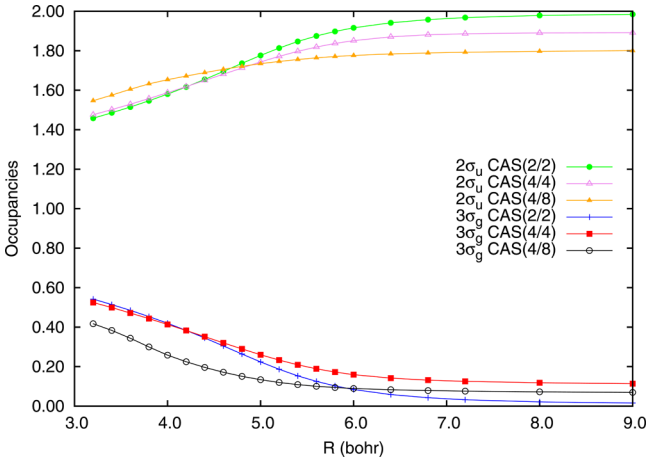

Figure 10. Occupation numbers of the $2\sigma_u$ (top) and $3\sigma_g$ (bottom) molecular orbitals with different active space.

internuclear distance confirms the multireference nature of the bond, and the fact that only two orbitals are strongly involved by quasi-degeneracy effects. Beyond the bond region (i.e., for $R > 6$ bohr) and with all active spaces, the occupation numbers are close to the RHF values (2 and 0 for the HOMO and the LUMO, respectively). This is particularly true for the CAS(2/2) values, because this space does not allow sp correlation on a single atom. The larger active spaces, on the other hand, do allow this type of correlation (CAS(4/8) to a larger extent than CAS(4/4)), and this accounts for the slight departure from RHF values of the occupation numbers in the large-distance region. The occupation numbers, on the other hand, start separating from the RHF values for $R < 6$ bohr. (This effect is slightly more pronounced for CAS(2/2) and CAS(4/4)) than for (CAS(4/8)). Close to equilibrium, in the cases of CAS(2/2) and CAS(4/4)), they are about 1.7 and 0.3 for $2\sigma_u$ and $3\sigma_g$, respectively. Notice that these values correspond to a wave function having a multireference character: in the case of the hydrogen dimer, for instance, this happens for an internuclear separation of about 2.4 times the equilibrium distance.

4.4. Total Position Spread of Be_2. In this section, we will use the total position spread (TPS) to characterize the nature of the wave function. The TPS denoted as Λ, is defined as the second moment cumulant of the electron positions of a molecular system. To compute it, one has to consider the

dx.doi.org/10.1021/jp503145u | J. Phys. Chem. A 2014, 118, 6664−6673

position operator and its tensorial square as described in ref.s.[13−19] We have

$$\hat{r}_\beta = \sum_{p=1}^{n} \hat{\beta}(p) \qquad \hat{r}_\beta \hat{r}_\gamma = \sum_{p,q=1}^{n} \hat{\beta}(p)\, \hat{\gamma}(q) \tag{5}$$

where the sums run over the n electrons and β, γ represent any of the Cartesian coordinates (x, y, and z). Once the position operator is evaluated using the respective one- and two-electron integrals, the Cartesian components of the tensor can be defined as follows:

$$\Lambda_{\beta\gamma} \equiv \langle \hat{r}_\beta \hat{r}_\gamma \rangle_c = \langle \Psi | \hat{r}_\beta \hat{r}_\gamma | \Psi \rangle - \langle \Psi | \hat{r}_\beta | \Psi \rangle \langle \Psi | \hat{r}_\gamma | \Psi \rangle \tag{6}$$

Roughly speaking, electrons that can easily move show a large value of $\mathbf{L}$ that can be interpreted as due to a wave function that is very delocalized and electrons are spread from their mean position in the molecular system.

In Figure 11 the $\mathbf{\Lambda}_\perp$ and $\mathbf{\Lambda}_\parallel$ components of the TPS are reported as a function of the internuclear distance for the Be_2

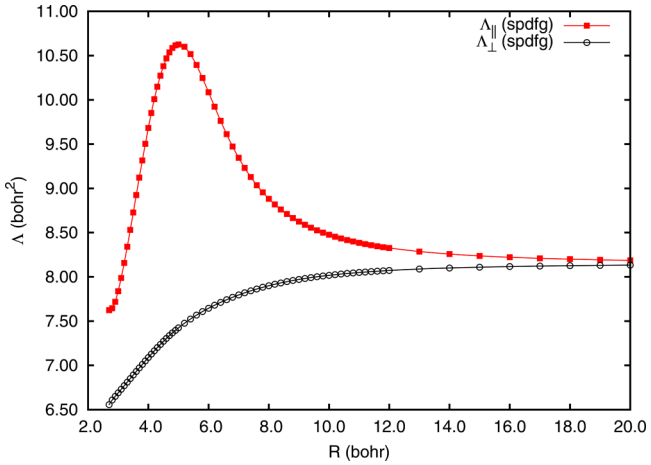

Figure 11. Total position spread computed for the $^1\Sigma_g^+$ ground state of beryllium at Full CI level of theory. The longitudinal component of the tensor is denoted as $\mathbf{\Lambda}_\parallel$ (red-square dashed line), and the perpendicular component is denoted as $\mathbf{\Lambda}_\perp$ (black-circles dashed lines).

molecule. It is remarkable that the TPS values in the atomic limit are larger than those in the region below 4 bohr. The latter results can be attributed to the increased nuclear effective charge affecting electrons at such distances (nuclei are closer to each other), which causes a spatial contraction of the orbitals in the direction perpendicular to the internuclear axis. Therefore, electrons are very localized in this molecular configuration and the TPS component more affected is the $\mathbf{\Lambda}_\perp$. Apart from this, the perpendicular component of the tensor does not show any special feature. Finally, this also indicates that electrons prefer to spread in the direction of the internuclear axis.

As concerns the longitudinal component $\mathbf{\Lambda}_\parallel$, it is an increasing function of R at short internuclear distances until it reaches a marked maximum just after equilibrium. As shown in refs 17 and 18, the TPS of diatomic molecules can be analyzed in terms of VB structures. A complete discussion of this point would require analyzing our wave functions in terms of VB structures, not an easy task, particularly for the large FCI wave functions. Here we limit ourselves to some qualitative considerations, leaving such analysis to a future work. One finds that the R dependence of the $\mathbf{\Lambda}_\parallel$ ionic structures is quadratically increasing, whereas that of the neutral ones is essentially negligible. On the other hand, in a molecule like Be_2 the relative weight of the ionic structures vanishes asymptotically at dissociation. Accordingly, the behavior of $\mathbf{\Lambda}_\parallel$ can be understood as a result of the interplay of these factors. In the small R region the weight of ionic structures is dominating, and the curve is increasing. By increasing R, the weight of the ionic structure rapidly decreases so the curve bends down and the ionic weight reaches zero at dissociation. In the cases previously studied[18] the maximum of the $\mathbf{\Lambda}_\parallel$ is associated with a change of the nature of the wave function. Here we note that Be_2, even if weakly bonded, shows the typical behavior of a covalent molecule and that the maximum falls at ≈5 bohr, not so far from the border of the BR. In ordinary covalent molecules (dissociating in open shell atoms) the wave function is essentially single-reference in the BR and becomes multi-reference in the AR (in terms of symmetry adapted MO's); here we have a similar transition but in the opposite direction.

5. CONCLUSIONS

The mechanism leading to the formation of a bond in beryllium dimer has emerged by comparing a series of CAS-SCF, CISD, MRCI, and FCI calculations, performed using different ANO basis sets. It has been shown that the main difficulty in describing this notoriously "difficult" bond arises from the different nature of the wave function in the minimum region and at dissociation. This implies that even small errors in the energy evaluation can give qualitatively wrong results.

However, the mechanism leading to the formation of a bond in the beryllium-dimer is relatively simple and can be summarized as follows:

1. The 1s core orbitals of the two beryllium atoms give rise to the $1\sigma_g$ and $1\sigma_u$ molecular orbitals (both doubly occupied) that do not participate to the bond mechanism.
2. In presence of a second Be atom, the quasi-degenerated 2s and 2p orbitals of each beryllium (hosting two electrons) form a pair of atomic sp hybrid orbitals on each atom, here denoted as ρ (inward pointing) and τ (outward pointing).
3. The four atomic hybrids give rise to four symmetry-adapted molecular orbitals. The ratio between the weights of s and p orbitals in these four MO's decreases as their energy increases. In ascending energy order, these orbitals are $2\sigma_g$, $2\sigma_u$, $3\sigma_g$, and $3\sigma_u$.
4. The two inward-pointing molecular orbitals ($2\sigma_g$ and $3\sigma_u$) have a clear bonding or antibonding character, respectively, because they are mainly located in the region between the two nuclei. These orbitals are either doubly occupied ($2\sigma_g$) or empty ($3\sigma_u$) in the reference wave function.
5. On the other hand, the two outer-pointing molecular edge orbitals are mainly located in the region external to the bond, and therefore are very close in energy. For this reason, their occupation numbers are not 2 or 0, but rather $2 - \delta$ (for $2\sigma_u$) and δ (for $3\sigma_g$), with $\delta = \delta(R)$.
6. Close to the equilibrium distance one has the following: $\delta \simeq 0.3$, the g orbitals have bonding character, whereas the u orbitals have antibonding character. This gives an overall "bond order" of about 0.3.
7. A bond order less than one-third of an ordinary single bond, indicates a very weak bond, which, however, is not

dx.doi.org/10.1021/jp503145u | J. Phys. Chem. A 2014, 118, 6664−6673

a dispersive interaction of van der Waals type. Rather, we consider the Be_2 bond as having a covalent nature as also suggested by the results of the total position spread.

This is our picture that gives a *qualitative description* of the bond formation in beryllium dimer. It is important to add the following to the previous points:

8. Because of the weakness of the bond, a very accurate balance of the different terms of dynamical/nondynamical correlation is required to have a *correct description* of the bond. In particular, because the electronic wave functions have a different nature at equilibrium and at dissociation, a balanced account of both orbital and correlation energy contributions in the two regions is particularly difficult to achieve. This explains why even sophisticated calculations can give completely wrong results, if they do not take into account this particular aspect of the Be_2 molecule.

In this paper we propose a new picture of the Be_2 bond, supported by high-quality ab initio calculations. In fact, as reflected by its weakness and length, this bond does not belong to anyone of the classes usually known in chemistry, neither can it be considered as a van der Waals interaction. In the framework of MO theory, a chemical bond is in general represented by a doubly occupied MO, associated with a single-reference wave function on top of which one adds nondynamical correlation to achieve quantitative accuracy. On the contrary, in this case, we have that a *two-reference picture* is needed to explain the bond already at a qualitative level. Therefore, the present work could be considered as an attempt to define a new type of chemical bond based on nondynamical correlation.

■ ASSOCIATED CONTENT

Supporting Information

The potential energy curves calculated at HF, CISD, and FCI using different basis sets, plots of the total energies obtained using an active space CAS(2/2) and its corresponding MRCI calculations, a list of vibrational levels of the potential curve obtained with FCI-spdf g basis, and output of Le Roy's program LEVEL 8.0 are given in the Supporting Information. This material is available free of charge via the Internet at http://pubs.acs.org/.

■ AUTHOR INFORMATION

Corresponding Author

*G. L. Bendazzoli: e-mail, gianluigi.bendazzoli@unibo.it.

Notes

The authors declare no competing financial interest.

■ ACKNOWLEDGMENTS

We thank prof. R. Cimiraglia of the University of Ferrara for using his 4-index transformation code. We thank the University of Toulouse and the French CNRS for financial support. We acknowledge the support of the Erasmus Mundus programme of the European Union (FPA 2010-0147). MEK acknowledges the ANR-DFG action ANR-11-INTB-1009 MITLOW for his PhD grant. GLB thanks the University of Bologna for support. Finally, we also thank the HPC resources of CALMIP under the allocation 2011-[p1048].

■ REFERENCES

(1) Vetere, V.; Monari, A.; Bendazzoli, G. L.; Evangelisti, S.; Paulus, B. Full configuration interaction study of the metal-insulator transition in model systems: Li_N linear chains (N = 2,4,6,8). *J. Chem. Phys.* **2008**, *128*, 024701/1−8.

(2) Salomonson, S.; Warston, H.; Lindgren, I. Many-Body Calculations of the Electron Affinity for Ca and Sr. *Phys. Rev. Lett.* **1996**, *76*, 3092−3095.

(3) Bondybey, V. E.; English, J. H. Laser vaporization of beryllium: Gas phase spectrum and molecular potential of Be_2. *J. Chem. Phys.* **1984**, *80*, 568−570.

(4) Bondybey, V. E. Electronic structure and bonding of Be_2. *Chem. Phys. Lett.* **1984**, *109*, 436−441.

(5) Bondybey, V. E. Laser-Induced Fluorescence and Bonding of Metal Dimers. *Science* **1985**, *227*, 125−131.

(6) Merritt, J. M.; Bondybey, V. E.; Heaven, M. C. Beryllium Dimer-Caught in the Act of Bonding. *Science* **2009**, *324*, 1548−1551.

(7) Patkowski, K.; Špirko, V.; Szalewicz, K. On the Elusive Twelfth Vibrational State of Beryllium Dimer. *Science* **2009**, *326*, 1382−1384.

(8) Meshkov, V. V.; Stolyarov, A. V.; Heaven, M. C.; Haugen, C.; LeRoy, R. J. Direct-potential-fit analyses yield improved empirical potentials for the ground $X^1\Sigma_g^+$ state of Be_2. *J. Chem. Phys.* **2014**, *140*, 064315/1−8.

(9) Patkowski, K.; Podeszwa, K.; Szalewicz, K. Interactions in Diatomic Dimers Involving Closed-Shell Metals. *J. Phys. Chem. A* **2007**, *111*, 12822−12838.

(10) Koput, J. The ground-state potential energy function of a beryllium dimer determined using the single-reference coupled-cluster approach. *Phys. Chem. Chem. Phys.* **2011**, *13*, 20311−20317.

(11) Sheng, X. W.; Kuang, X. Y.; Li, P.; Tang, K. T. Analyzing and modeling the interaction potential of the ground-state beryllium dimer. *Phys. Rev. A* **2013**, *88*, 022517/1−6.

(12) Helal, W.; Evangelisti, S.; Leininger, T.; Monari, A. A FCI benchmark on beryllium dimer: The lowest singlet and triplet states. *Chem. Phys. Lett.* **2013**, *568*, 49−54.

(13) Bendazzoli, G. L.; Evangelisti, S.; Monari, A. Full-configuration-interaction study of the metal-insulator transition in a model system: H_n linear chains n = 4,6,...,16. *Int. J. Quantum Chem.* **2011**, *111*, 3416−3423.

(14) Ángyán, J. G. Linear Response and Measures of Electron Delocalization in Molecules. *Curr. Org. Chem.* **2011**, *15*, 3609−3618.

(15) Bendazzoli, G. L.; Evangelisti, S.; Monari, A. Asymptotic analysis of the localization spread and polarizability of 1-D noninteracting electrons. *Int. J. Quantum Chem.* **2012**, *112*, 653−664.

(16) Giner, E.; Bendazzoli, G. L.; Evangelisti, S.; Monari, A. Full-configuration-interaction study of the metal-insulator transition in model systems: Peierls dimerization in H_n rings and chains. *J. Chem. Phys.* **2013**, *138*, 074315/1−8.

(17) Angeli, C.; Bendazzoli, G. L.; Evangelisti, S. The localization tensor for the H_2 molecule: closed formulae for the Heitler-London and related wavefunctions and comparison with full configuration interaction. *J. Chem. Phys.* **2013**, *138*, 054314/1−9.

(18) Brea, O.; El Khatib, M.; Angeli, C.; Bendazzoli, G. L.; Evangelisti, S.; Leininger, T. Behavior of the Position-Spread Tensor in Diatomic Systems. *J. Chem. Theory Comput.* **2013**, *9*, 5286−5295.

(19) El Khatib, M.; Leininger, T.; Bendazzoli, G. L.; Evangelisti, S. Computing the Position-Spread tensor in the CAS-SCF formalism. *Chem. Phys. Lett.* **2014**, *591*, 58−63.

(20) Bendazzoli, G. L.; El Khatib, M.; Evangelisti, S.; Leininger, T. The total Position Spread in mixed-valence compounds: A study on the H_4^+ model system. *J. Comput. Chem.* **2014**, *35*, 802−808.

(21) Koput, J.; Peterson, K. A. Ab initio prediction of the potential energy surface and vibration-rotation energy levels of BeH_2. *J. Chem. Phys.* **2006**, *125*, 044306/1−7.

(22) Roos, B. O.; Taylor, P. R.; Siegbahn, P. E. M. A complete active space SCF method (CASSCF) using a density matrix formulated super-CI approach. *Chem. Phys.* **1980**, *48*, 157−173.

(23) Werner, H.-J.; Knowles, P. J. A second order multiconfiguration SCF procedure with optimum convergence. *J. Chem. Phys.* **1985**, *82*, 5053−5063.
(24) Knowles, P. J.; Werner, H.-J. An efficient second-order MC SCF method for long configuration expansions. *Chem. Phys. Lett.* **1985**, *115*, 259−267.
(25) Werner, H.-J.; Knowles, P. J. An efficient internally contracted multiconfiguration−reference configuration interaction method. *J. Chem. Phys.* **1988**, *89*, 5803−5814.
(26) Knowles, P. J.; Werner, H.-J. An efficient method for the evaluation of coupling coefficients in configuration interaction calculations. *Chem. Phys. Lett.* **1988**, *145*, 514−522.
(27) MOLPRO is a package of ab initio programs written by Werner, H.-J.; Knowles, P. J. with contribution from Almlöf, J.; Amos, R. D.; Berning, A.; Deegan, M. J. O.; Eckert, F.; Elbert, S. T.; Hampel, C.; Lindh, R.; et al.
(28) NEPTUNUS is a FORTRAN code for the calculation of FCI energies and properties written by Bendazzoli, G. L. and Evangelisti, S. with contributions from Gagliardi, L.; Giner, E.; Monari, A.; Verdicchio, M.
(29) Bendazzoli, G. L.; Evangelisti, S. A vector and parallel full configuration interaction algorithm. *J. Chem. Phys.* **1993**, *98*, 3141−3150.
(30) Gagliardi, L.; Bendazzoli, G. L.; Evangelisti, S. Direct-list algorithm for configuration interaction calculations. *J. Comput. Chem.* **1997**, *18*, 1329−1343.
(31) Aquilante, F.; De Vico, L.; Ferré, N.; Ghigo, G.; Malmqvist, P.-Å; Neogrády, P.; Pedersen, T. B.; Pitoňák, M.; Reiher, M.; Roos, B. O.; et al. MOLCAS 7: The Next Generation. *J. Comput. Chem.* **2010**, *31*, 224−247.
(32) *DALTON*, a Molecular Electronic Structure Program, Release 2.0 (2005): see http://www.kjemi.uio.no/software/dalton/dalton.html.
(33) Angeli, C.; Bendazzoli, G. L.; Borini, S.; Cirmiraglia, R.; Emerson, A.; Evangelisti, S.; Maynau, D.; Monari, A.; Rossi, E.; Sanchez-Marìn, J.; et al. The problem of interoperability: A common data format for quantum chemistry codes. *Int. J. Quantum Chem.* **2007**, *107*, 2082−2091.
(34) Borini, S.; Monari, A.; Rossi, E.; Tajti, A.; Angeli, C.; Bendazzoli, G. L.; Cirmiraglia, R.; Emerson, A.; Evangelisti, S.; Maynau, D.; et al. FORTRAN Interface for Code Interoperability in Quantum Chemistry: The Q5Cost Library. *Chem. Inf. Model.* **2007**, *47*, 1271−1277.
(35) Rampino, S.; Monari, A.; Rossi, E.; Evangelisti, S.; Laganà, A. A priori modeling of chemical reactions on computational grid platforms: Workflows and data models. *Chem. Phys.* **2012**, *398*, 192−198.
(36) Rossi, E.; Evangelisti, S.; Laganà, A.; Monari, A.; Rampino, S.; Verdicchio, M.; Baldridge, K.; Bendazzoli, G. L.; Borini, S.; Cimiraglia, R.; et al. Code interoperability and standard data formats in quantum chemistry and quantum dynamics: The Q5/D5Cost data model. *J. Comput. Chem.* **2014**, *35*, 611−621.
(37) Le Roy, R. J. LEVEL 8.0: A Computer Program for Solving the Radial Schrödinger Equation for Bound and Quasibound Levels *University of Waterloo Chemical Physics Research Report CP-663* **2007**; see http://leroy.uwaterloo.ca/programs/.
(38) Lepetit, M.; Malrieu, J. P. Interaction of s^2 pairs in Be_2 and C_2: The UHF instability, symptom of an atomic promotion. *Chem. Phys. Lett.* **1990**, *169*, 285−291.
(39) Li, P.; Ren, J.; Niu, N.; Tang, K. T. Corresponding States Principle for the Alkaline Earth Dimers and the van der Waals Potential of Ba_2. *J. Phys. Chem. A* **2011**, *115*, 6927−6935.
(40) Pastore, M.; Monari, A.; Angeli, C.; Bendazzoli, G. L.; Cimiraglia, R.; Evangelisti, S. A theoretical study of Be_N linear chains: Variational and perturbative approaches. *J. Chem. Phys.* **2009**, *131*, 034309/1−12.